ACS APPLIED MATERIALS & INTERFACES

Letter

www.acsami.org

# Solvothermal Synthesis of Microporous, Crystalline Covalent Organic Framework Nanofibers and Their Colorimetric Nanohybrid Structures

Wei Huang, Yi Jiang, Xiang Li, Xiaojuan Li, Jianying Wang, Qi Wu, and Xikui Liu*

College of Polymer Science and Engineering, Sichuan University, Chengdu 610065, People's Republic of China

Supporting Information

**ABSTRACT:** This paper reports a facile solvothermal approach for the design and synthesis of novel crystalline COF nanofibers with amazing properties. An interesting morphological transformation from microsphere to nanofibers was observed, which could be supported by the unique dissolution-recrystallization mechanism due to the reversible nature of dynamic imine bonding. Interestingly, it was also found that the COF nanofibers could epitaxial grow on the aramid microfiber surface. This functional nanocomposite showed an interesting colorimetric humidity-responsive behavior. Our study provides a general methodology for the fabrication of COFs with designated micronanostructures and has more implications on their applications in catalyst and sensors.

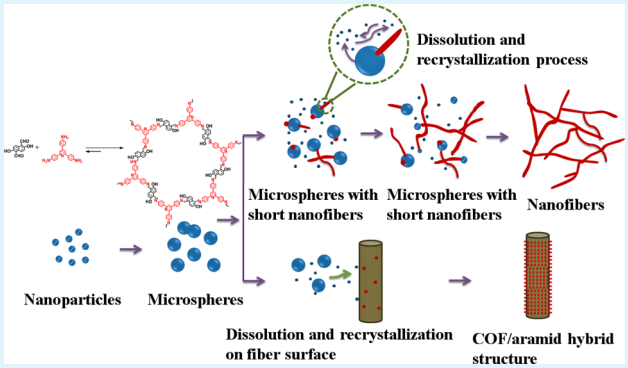


**KEYWORDS:** *covalent organic frameworks, nanofibers, solvothermal synthesis, dissolution–recrystallization, nanohybrid*

## 1. INTRODUCTION

Since the first breakthrough for the synthesis of crystalline covalent organic frameworks (COFs) in 2005,[1] research on this filed has attracted much attention because of their promising potential applications as gas storage, catalyst, and photoelectricity.[1−8] Compared with inorganic zeolites and metal organic frameworks (MOFs), COFs are constructed solely from lightweight elements linked via strong covalent bonds, which makes them extremely low density and robust.[9,10] The successful application of network materials depends not only on their special chemical structures but also on their morphologies, sizes and architectures.[10] To date, however, most of the COFs obtained were irregular crystal powders except for some rare samples with special morphology, such as nanobelt and nanocubes.[5,11−13] Although great achievements have been made in synthesizing MOFs with arbitrary dimensions, morphologies, and increased complexity, we are still facing big challenges in obtaining shape-tailored COFs for advanced applications.

Reversible nature of covalent bond has been proved of vital importance for the formation of ordered polymeric frameworks, since it allows for error-checking during synthesis, on the basis of which, composite exchange and morphology transformation can be realized. For example, Yaghi et al. synthesized crystalline covalent organic frameworks based on dynamic borate ester bonding.[1−3] Kuhn and Antonietti et al. further revealed that the high-temperature dynamic polymerization of aromatic nitriles in molten salt resulted in crystalline triazine-based frameworks.[22] Recently, Kubo et al. reported an interesting morphology transformation from microspheres to microribbons for dynamic polymer with the reversible borate ester bonds.[15] Recently, we found that this reversible nature of covalent bonds can also be extended to control the formation and morphology evolution of aromatic polymers at microscale which has been rarely observed in classical polymeric materials without dynamic covalent bonds.[16,17] However, the mechanism of dynamic covalent chemistry controlled morphology behavior is still under investigation and many interesting aspects remain largely unexplored.

Herein, taking advantage of the dynamic nature of imine bonds, we present a facile solvothermal route for the synthesis of rarely reported uniform crystalline COF nanofibers. The time-dependent growth of COF nanofibers and a very interesting morphology transformation process from nanoparticles to nanofibers was observed, which is controlled by a novel dissolution–recrystallization growth mechanism enabled by the unique reversibility of imine (C═N) bonds. This particular transformation process can successfully applied to the fabrication of complex COF nanohybrid structures. When foreign nucleate agents were added in the solvothermal system, crystalline COF nanohybrid structures can be obtained, which provides a facile and unique strategy for preparing COFs with well-defined micronanostructures and paves the way to the understanding of growth mechanism of COFs (Scheme 1).

## 2. EXPERIMENTAL SECTION

**2.1. Monomer Synthesis.** 2,6-Dihydroxynaphthalene-1,5-dicarbaldehyde (DHNDA) and 2,4,6-tris(4-aminophenyl)-

Received: July 3, 2013
Accepted: August 9, 2013
Published: August 9, 2013

   dx.doi.org/10.1021/am402649g | ACS Appl. Mater. Interfaces 2013, 5, 8845−8849

**Scheme 1. Synthesis of COFs by Condensation of DHNDA and TAPP and the Tautomerization between Enol and Keto Forms**

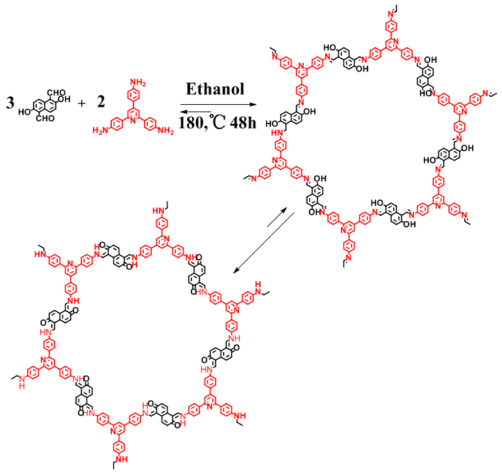


pyridine (TAPP) were prepared and purified following literature procedures (see the Supporting Information). Other chemicals and solvent were purchased and purified according to standard procedures.

**2.2. Solvothermal Synthesis of Microporous, Crystalline COF Nanofibers.** A mixture of DHNDA (120 mg, 0.56 mmol) and TAPP (130.4 mg, 0.37 mmol) in anhydrous alcohol (50 mL) in a Teflon-lined autoclave was sonicated for 15 min at room temperature. Then the autoclave was transferred in an oven and heated at 180 °C for 48 h, the precipitation was collected by filtration and washed with dioxane and acetone, and dried at 150 °C under vacuum for 24 h, yield ca. 90%.

**2.3. Solvothermal Synthesis of COF/Aramid Hybrid Material.** The COF formed at the initial solvothermal process were filtrated out and redispersed in 50 mL fresh anhydrous alcohol with a piece of aramid fabric (1 × 1 $cm^2$) in a Teflon-lined autoclave, the autoclave was transferred in an oven and heated to 180 °C for 48 h. After that, the COF/aramid fabric was washed with THF and dried at 150 °C under vacuum for 24 h to give a light yellow colored nanohybrid fabric.

**2.4. Characterization.** FT-IR spectra were measured with a Nicolet 560 spectrometer. $^1$H NMR spectra was recorded in DMSO-$d_6$ solution on a 400 MHz Bruker Avance 400 NMR spectrometer. Solid-state nuclear magnetic resonance (NMR) spectra were recorded on a Bruker Avance III 500 MHz with a standard 4-mm Bruker MAS Probe at a sample spinning rate of 8.0 kHz. Element analysis was carried out on a Euro EA 3000 elemental analyzer. Powder X-ray diffraction (PXRD) data were collected with an X'Pert Pro MPD diffractometer operated at 30 KV and 15 mA with Cu K$\alpha$ radiation, from $2\theta$ = 1.5−40° with a scanning rate of 1°/min. Scanning electron microscopy (SEM) was conducted with an Inspect F SEM at an accelerating voltage of 20KV. Transmission electron microscopy observations were performed with a JEM 100CX II transmission electron microscope at an accelerating voltage 80 KV. The nitrogen absorption and desorption isotherms were measured at 77 K using a Tristar system. The sample was degassed at 150 °C for 10 h before the measurement. Surface area was calculated from the adsorption data using Brunauer−Emmett−Teller (BET) method. The pore width distribution curves were obtained from the adsorption branch using nonlocal density functional theory (NLDFT) method. The thermal property was measured using a Thermo gravimetric analysis (TGA) instruments (SDT Q600) over the temperature range of 33−800 °C with a heating rate of 10 °C/min.

## 3. RESULTS AND DISCUSSION

The successful preparation of the COFs was confirmed by FT-IR spectroscopy and $^{13}$C NMR technology. Two shoulder bands at 1617 $cm^{-1}$ and 1629 $cm^{-1}$, which are attributed to C═N stretching in enol form and C═O stretching in keto form, respectively, can be clearly identified (see Figures S1 and S2 in the Supporting Information). The absence of the peak at 193 ppm (aldehyde carbonyl carbon of DHNDA) in the $^{13}$C NMR spectrum and the peaks appearing at 184 and 153 ppm corresponding to the carbonyl carbon and imine carbon in keto form and enol form also indicates the total conversion of starting monomers (see Figure S5 in the Supporting Information). Elemental analysis found: C, 76.33%; N, 8.53%; H, 5.26%, which was consistent with the calculated values: C, 79.10%; N, 9.00%; H, 4.18%.

The products are composed of a large quantity of uniform nanofibers with lengths of up to tens of micrometers (Figure 1a), such a fibrous morphology has been rarely reported in

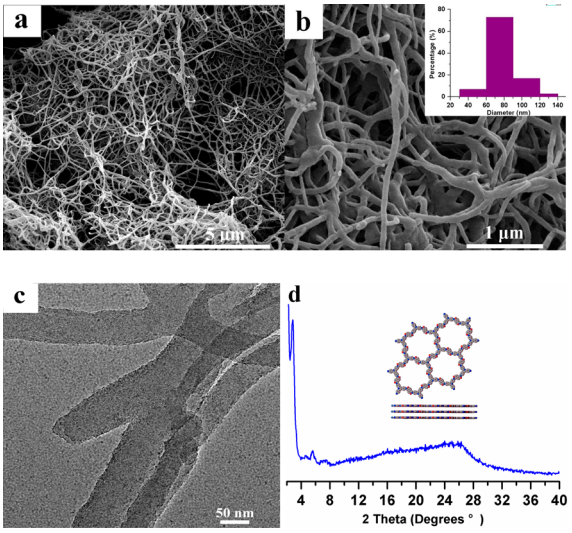


**Figure 1.** (a, b) SEM and (c) TEM images and (d) PXRD pattern of the synthesized COF nanofibers.

crystalline COF systems. Besides, the histogram of about 100 nanofibers reveals that the nanofibers are uniform with diameter about 80 nm (Figure 1b). Most of the nanofibers have branched structure, which could also be confirmed by TEM image (Figure 1c).

The powder X-ray diffraction (PXRD) pattern of the product exhibits an intense peak at ∼2.7° with the *d*-spacing of ∼32.6 Å, which corresponds to the reflection from (100) plane, indicating the COF nanofiber has a long-rang molecular ordering (Figure 1d). The broad peak at ∼25.4° is due to the reflection from the (001) plane, which corresponds to interlayer distances about ∼3.5 Å. Furthermore, several weaker diffraction peaks also be observed at $2\theta$ = 4.5, 5.3, and 7.0°, which are attributed to the (110), (200), and (210) planes, respectively. The PXRD profile was indexed on a primitive hexagonal unit cell and refined using the Pawley method in the Reflex module of Material Studio (Ver. 4.0),[18] yield cell parameters $a = b$ = 37.30 Å, $c$ = 3.47 Å (residuals: $R_p$ = 3.48%

and $R_{wp}$ = 4.58%, respectively) (see Figure S4 in the Supporting Information).

A totally unexpected morphological transformation was observed when tracing the morphology evolution process. The reaction between DHDNA and TAPP quickly leading to precipitates of irregular nanoparticles with diameter about 40 nm (Figure 2a), these nanoparticles gradually fused to

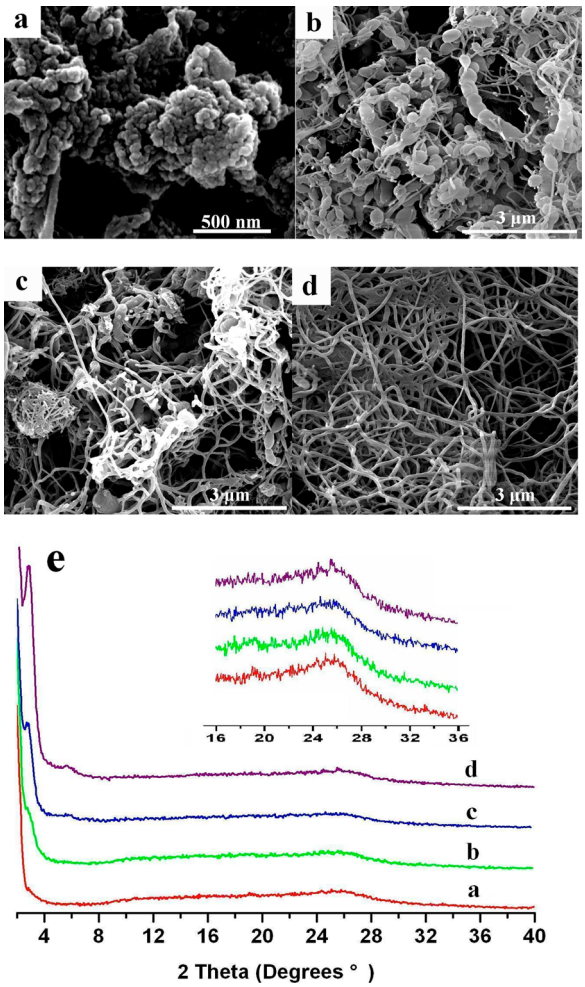


**Figure 2.** SEM images of samples obtained from different reaction times: (a) 85 °C for 2 h, (b) stop reaction when reach to 180 °C, (c) 180 °C for 5 h, and (d) 180 °C for 24 h, and (e) their corresponding PXRD patterns.

microspheres with diameter about 350 nm (Figure 2b), some short nanofibers can be found on the surface of microspheres. Unexpectedly, with increasing the solvothermal reaction time, the nanofibers grew longer and longer; meanwhile, the microspheres become smaller and smaller (Figure 2c). After 24 h, the microspheres can be scarcely observed, only uniform nanofibers can be found (Figure 2d). The corresponding PXRD pattern of the products clearly reflects the changes of the crystallinity from amorphous to highly crystalline along with the small angle area intensity gradually increasing (Figure 2e). Meanwhile, the FT-IR spectra of these samples have no significant difference (see Figure S3 in the Supporting Information), which indicates this transformation is mainly driven by the increased crystallinity.

The transformation from microsphere to nanofiber is totally unexpected. Based on the above results, we speculate the transformation can be rationally expressed as a unique dissolution−recrystallization process: First, the condensation reaction between DHNDA and TAPP quickly gives polyimine frameworks with irregular nanoparticles through a homogeneous nucleation process, these nanoparticles quickly aggregate into uniform microspheres with diameter about 340 nm. With increasing the reaction time at 180 °C, the microspheres partially dissolve into the solution due to the unique reversibility of dynamic imine bonds. These dissolved fragments further react and recrystallize onto the small high-energy nucleate sites of microspheres, the nucleation growth likes to take along the 1D direction. The continuous dissolution of the microspheres finally leads to the formation of crystalline COF nanofibers (Scheme 2).

**Scheme 2. Formation of COF Nanofibers through Dynamic Imine Chemistry Enabled by Dissolution-Recrystallization Process**

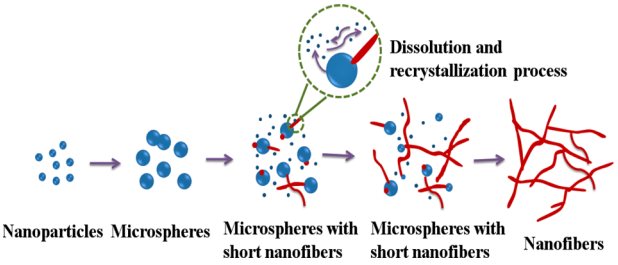


Such a dissolution−recrystallization process, first proposed in inorganic materials,[19,20] has been rarely reported in polymeric systems. We believed that the reversibility of dynamic imine bonds is responsible for this process.[1,14] To test the validity of this mechanism, we conducted control experiments. The microspheres formed at the initial stage were filtered out of the growth solution and then washed with ethanol to remove the unreacted monomers and oligomers. The microspheres were then dispersed in 50 mL fresh ethanol and solvothermal treatment at 180 °C for 48 h. After the second-time solvothermal treatment, pure and uniform crystalline COF nanofibers as the only product were also observed (Figure 3),

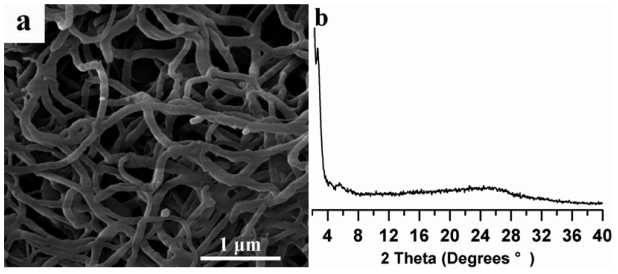


**Figure 3.** (a) SEM image and (b) PXRD pattern of the nanofibers obtained from second-time solvothermol treatment.

no microsphere residues can be found. This definitely confirms that the nanofibers are formed through a dissolution−recrystallization transformation process instead of from the unreacted monomers in the solution.

The isotherm curves of the nitrogen sorption exhibit a typical IVtype reversible isotherm sorption character indicating mesoporous character of the COF nanofibers (Figure 4a). The Brunauer−Emmett−Teller (BET) surface area and the

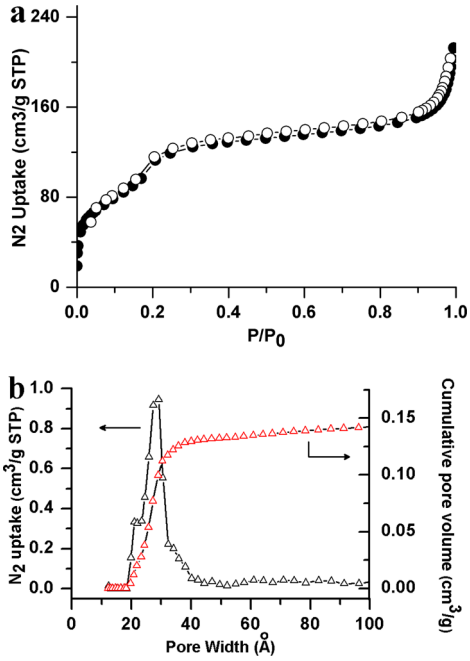


**Figure 4.** (a) Nitrogen adsorption/desorption isotherms of COF nanofibers and (b) pore width distribution curves.

pore volume calculated from the sorption profile are 416 $m^2/g$ ($0.05 < P/P_0 < 0.2$) and 0.33 $cm^3/g$ ($P/P_0 = 0.99$), respectively, which is similar to the reported values of most two-dimensional COFs.[3,4] The pore size distribution plots of COF nanofibers revealed a row pore width distribution at ~2.9 nm (Figure 4b). The thermogravimetric analysis (TGA) shows that COFs nanofibers is stable up to 400 °C (see Figure S7 in the Supporting Information) with carbon yield of 51% upon heating to 800 °C, thus confirming their excellent thermal stability.

One-dimensional organic/inorganic hybrid materials have attracted much attention because of their outstanding optical and electrical properties.[21] Given the unique dissolution−recrystallization mechanism, the formation of COF hybrid structures is expected through adding some foreign nucleate agents. As a proof-concept experiment, aramid fabric was chosen due to its good nucleation ability for many kinds of polymers.[22] The initially formed microspheres and a piece of aramid fabric (1 × 1 $cm^2$) were dispersed in fresh alcohol followed solvothermal treatment. The SEM images clearly revealed that large amounts of very short COF nanofibers with diameter about 35 nm were formed on the surface of aramid fibers (Figure 5). The formation of this hybrid structure further verified the proposed dissolution- recrystallization mechanism.

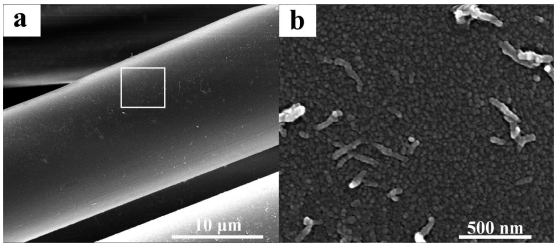


**Figure 5.** (a) SEM image and (b) enlarged SEM image of the surface of COF/aramid nanohybrid structure.

Interestingly, the obtained COF/aramid nanohybrid material shows a humidity-responsive color-changing property. In a dry atmosphere (relative humidity (R.H) 20%), the fabric is light yellow, the color of the fabric gradually changed from light red to dark red with increasing R.H from 20% to 100% (Figure 6).

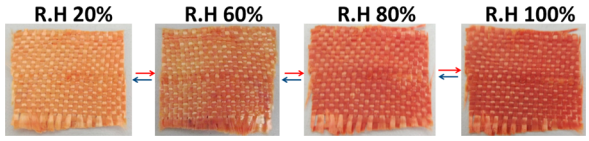


**Figure 6.** Digital photographs of the reversible humidity-responsive color-changesof COF/aramid fabrics under different relative humidity.

Also, the color-changing process is reversible and repeatable, which provides a simple naked-eye detection for the environmental humilities. The transformation of isomers between enol form and keto form promoted by moisture may be the most reasonable explanation.[23] Such a low-cost and scalable method for the fabrication of colorimetric moisture-sensitive fabrics will have great advantage for its further applications.

## 4. CONCLUSION

In summary, we reported our work on the road to some basic understanding about the mechanisms behind the morphology control of COFs and their hybrid structures. Uniform crystalline COF nanofibers were successfully synthesized for the first time, through a facile solvothermal process, and a detail observation revealed an interesting morphological transformation from microsphere to nanofibers, the formation of COF nanofibers is through an interesting dissolution-recrystallization process due to the reversable nature of dynamic imine bonds. This transformation can successfully applied to the fabrication of complex COF nanohybrid structures using aramid fiber as foreign nucleate agent. Besides, this COF naohybrid structure showed an interesting reversible colorimetric humidity-sensitive property. It is still difficult to give a full picture of this dynamic covalent chemistry enabled by dissolution-recrystallization process for the formation of crystalline COFs nanofibers, and a tremendous amout of work remains to be done. We believe that our study provides a generally methodology for the fabrication of COFs with designated micronanostructures, which will surely extend their applications such as catalysis, membrane separations, and sensors.

## ■ ASSOCIATED CONTENT

### Ⓢ Supporting Information

FT-IR spectrum, molecular modul, $^{13}C$ NMR spectra, additional gas absorption data, TGA and DTG profiles, SEM and XRD spectra. This material is available free of charge via the Internet at http://pubs.acs.org/.

## ■ AUTHOR INFORMATION

### Corresponding Author

*E-mail: xkliu@scu.edu.cn.

### Notes

The authors declare no competing financial interest.

## ■ ACKNOWLEDGMENTS

We are grateful for the financial support from the National Natural Science Foundation of China (20974069, 21174089), and Sichuan University (0082204121012).

## ■ REFERENCES

(1) Cote, A. P.; Benin, A. I.; Ockwig, N. W.; O'Keeffe, M.; Matzger, J.; Yaghi, O. M. *Science* **2005**, *310*, 1166−1170.
(2) Uribe-Romo, F. J.; Doonan, C. J.; Furukawa, H.; Oisaki, K.; Yaghi, O. M. *J. Am. Chem. Soc.* **2011**, *133*, 11478−11481.
(3) Wan, S.; Gandara, F.; Asano, A.; Furukawa, H.; Saeki, A.; Dey, S. K.; Liao, L.; Ambrogio, M. W.; Botros, Y. Y.; Duan, X. F.; Seki, S.; Stoddart, J. F.; Yaghi, O. M. *Chem. Mater.* **2011**, *23*, 4094−4097.
(4) Ding, S. Y.; Gao, J.; Wang, Q.; Zhang, Y.; Song, W. G.; Shu, C. Y.; Wang, W. *J. Am. Chem. Soc.* **2011**, *133*, 19816−19822.
(5) Wan, S.; Guo, J.; Kim, J.; Ihee, H.; Jiang, D. L. *Angew. Chem.* **2008**, *120*, 8958−8962.
(6) Feng, X.; Chen, L.; Honsho, Y.; Saengsawang, O.; Liu, L. L.; Wang, L.; Saeki, A.; Irle, S.; Seki, S.; Dong, Y. P; Jiang, D. L. *Adv. Mater.* **2012**, *24*, 3026−3031.
(7) Jin, S. B.; Ding, X. S.; Feng, X.; Supur, M.; Furukawa, K.; Takahashi, S.; Addicoat, M.; El-Khouly, M. E.; Nakamura, T.; Irle, S.; Fukuzumi, S.; Nagai, A.; Jiang, D. L. *Angew. Chem., Int. Ed.* **2013**, *52*, 2017−2021.
(8) El-Kaderi, H. M.; Hunt, J. R.; Mendoza-Cortes, J. L.; Cote, A. P.; Taylor, R. E.; O'Keeffe, M.; Yaghi, O. M. *Science* **2007**, *316*, 268−272.
(9) Ding, S. Y.; Wang, W. *Chem. Soc. Rev.* **2013**, *42*, 548−568.
(10) Hu, J. T.; Odom, T. W.; Lieber, C. M. *Acc. Chem. Res.* **1999**, *32*, 435−445.
(11) Nagai, A.; Guo, Z. Q.; Feng, X.; Jin, S. B.; Chen, X.; Ding, X. S.; Jiang, D. L. *Nat. Commun.* **2011**, *2*, 536−543.
(12) Feng, X.; Chen, L.; Dong, Y. P.; Jiang, D. L. *Chem. Commun.* **2011**, *47*, 1979−1981.
(13) Kandambeth, S.; Mallick, A.; Lukose, B.; Mane, M. V.; Heine, T.; Banerjee, R. *J. Am. Chem. Soc.* **2012**, *134*, 19524−19527.
(14) Feng, X.; Ding, X. S.; Jiang, D. L. *Chem. Soc. Rev.* **2012**, *41*, 6010−6022.
(15) Nishiyabu, R.; Teraoka, S.; Matsushima, Y.; Kubo, Y. *ChemPlusChem.* **2012**, *77*, 201−209.
(16) Yan, Y. Z.; Chen, L.; Dai, H. J.; Chen, Z. H.; Li, X.; Liu, X. K. *Polymer* **2012**, *53*, 1611−1616.
(17) Chen, Z. H.; Jiang, Y.; Chen, L.; Huang, W.; Li, X.; Li, X. J.; Liu, X. K. *Polym. J.* DOI: 10.1038/pj.2013.23. Advance online publication 13 March 2013. Access date: 7-Aug-**2013**
(18) *Materials Studio Release Notes*, version 4.0; Accelrys Software Inc.: San Diego, CA, 2006. Access date: 7-Aug-2013.
(19) Wang, Z. H.; Liu, J. W.; Chen, X. Y.; Wan, J. X.; Qian, Y. T. *Chem.—Eur. J.* **2005**, *11*, 160−163.
(20) Xi, G. C.; Xiong, K.; Zhao, Q. B.; Zhang, R.; Zhang, H. B.; Qian, Y. T. *Crys. Growth & Des.* **2006**, *6*, 577−582.
(21) Zheng, H. Y.; Li, Y. J.; Liu, H. B.; Yin, X. D.; Li, Y. L. *Chem. Soc. Rev.* **2011**, *40*, 4506−4524.
(22) Kuhn, P.; Forget, A.; Su, D. S.; Thomas, A.; Antonietti, M. *J. Am. Chem. Soc.* **2008**, *130*, 13333−13337.
(23) Ziotek, M.; Kubicki, J.; Maciejewski, A.; Naskrcki, R.; Grabowska, A. *J. Chem. Phys.* **2006**, *124*, 124518−124527.